Suppression of Ewing's Sarcoma Tumor Growth, Tumor Vessel Formation, and Vasculogenesis Following Anti–Vascular Endothelial Growth Factor Receptor-2 Therapy

Zhichao Zhou,[1] Marcela F. Bolontrade,[1] Krishna Reddy,[1] Xiaoping Duan,[1] Hui Guan,[1] Ling Yu,[1] Daniel J. Hicklin,[2] and Eugenie S. Kleinerman[1]

Abstract

Purpose: We previously showed that bone marrow cells participate in new tumor vessel formation in Ewing's sarcoma, and that vascular endothelial growth factor 165 ($VEGF_{165}$) is critical to this process. The purpose of this study was to determine whether blocking VEGF receptor 2 (VEGFR-2) with DC101 antibody suppresses tumor growth, reduces tumor vessel formation, and inhibits the migration of bone marrow cells into the tumor.

Experimental Design: An H-2 MHC-mismatched bone marrow transplant Ewing's sarcoma mouse model was used. Bone marrow cells from CB6F1 (MHC H-$2^{b/d}$) mice were injected into irradiated BALB/cAnN mice (MHC H-2^{d}). TC71 Ewing's sarcoma cells were s.c. injected 4 weeks after the bone marrow transplantation. Mice were then treated i.p. with DC101 antibody or immunoglobulin G (control) twice a week for 3 weeks starting 3 days after tumor cell injection.

Results: DC101 antibody therapy significantly reduced tumor growth and tumor mean vessel density ($P < 0.05$) and increased tumor cell apoptosis. Decreased bone marrow cell migration into the tumor was also shown after DC101 therapy as assessed by the colocalization of H-$2K^{b}$ and CD31 using immunohistochemistry. DC101 inhibited the migration of both human and mouse vessel endothelial cells *in vitro*.

Conclusion: These results indicated that blocking VEGFR-2 with DC101 antibodies may be a useful therapeutic approach for treating patients with Ewing's sarcoma.

Solid tumors require development and expansion of a vascular network for nourishment and waste disposal to support their growth. Angiogenesis was initially regarded as the sole mechanism by which tumor vessels expand. However, other mechanisms are involved in the expansion of the tumor vascular network. For example, tumors such as gliomas use preexisting vessels to increase tumor vascularity through a mechanism called vessel cooption (1). Another example is aggressive uveal and epithelial melanomas that promote the expansion of their vascular network partly by arranging tumor cells into functional vascular channels through a mechanism referred to as vasculogenic mimicry. This mechanism has also been shown in ovarian and prostate cancer (2–4). Both angiogenesis and vascular mimicry occur as a result of stimulation of the cells in the immediate tumor area. By contrast, vasculogenesis involves the formation of blood vessels from endothelial precursor cells that are induced to migrate and home into the area of vessel formation. Vasculogenesis is a process originally described during prenatal development. A vasculogenesis-like mechanism, which recruits nonlocal cells to the area of new vessel formation, has been shown to occur during postnatal life. This can take place under both physiologic and pathologic conditions such as wound healing, the revascularization of ischemic tissues, or tumor formation. We have shown that a vasculogenesis-like component is operational during the development of Ewing's sarcoma (5, 6). This vasculogenesis-like process involves the active participation of bone marrow (BM) cells. We showed that BM-derived cells not only reconstituted the hematopoietic system in mice after lethal irradiation, but also contributed to the new vessel formation during Ewing's sarcoma tumor growth (5, 6).

Multiple growth factors including vascular endothelial growth factor (VEGF) affect tumor development. VEGF has been shown to be up-regulated in several tumor models and in cancer patients' samples (7, 8). The regulation of VEGF expression is tightly controlled during development and postnatal life and affects multiple functions on both endothelial and other cell types (9, 10). VEGF also acts as a survival factor for normal endothelial cells, hence the significance of its up-regulation during tumor formation. Ewing's sarcoma cells overexpress VEGF, with an isoform switching from the

Authors' Affiliations: [1]Division of Pediatrics, The University of Texas M. D. Anderson Cancer Center, Houston, Texas; and [2]ImClone Systems, Inc., New York, New York

Received 1/17/07; revised 5/8/07; accepted 5/14/07.

Grant support: National Cancer Institute grant CA 103986 (E.S. Kleinerman), The Elliot Kayton Memorial Fund (E.S. Kleinerman), and National Cancer Institute core grant CA16672.

The costs of publication of this article were defrayed in part by the payment of page charges. This article must therefore be hereby marked *advertisement* in accordance with 18 U.S.C. Section 1734 solely to indicate this fact.

Note: M.F. Bolontrade's current address: Foundation Institute Leloir-CONICET, Buenos Aires, Argentina.

Requests for reprints: Eugenie S. Kleinerman, Division of Pediatrics, Unit 87, The University of Texas M. D. Anderson Cancer Center, 1515 Holcombe Boulevard, Houston, TX 77030. Phone: 713-792-8110; Fax: 713-794-5042; E-mail: ekleiner@mdanderson.org.

doi:10.1158/1078-0432.CCR-07-0133

extracellular matrix–bound 189 isoform to the smaller and more soluble 165 isoform (6). We previously showed that $VEGF_{165}$ is a chemoattractant for BM-derived cells *in vivo* using VEGF-containing Matrigel plugs (5). We also showed that specifically inhibiting $VEGF_{165}$ using small interfering RNA (siRNA) technology resulted in decreased BM cell migration into the tumor, fewer tumor vessels, and slower tumor growth (11).

In this study, we showed that inhibiting VEGF activity by blocking the VEGF receptor 2 (VEGFR-2) inhibits tumor growth, mean microvessel density (MVD), and the recruitment of BM-derived cells into the tumor site. These results confirmed that VEGF is a crucial factor during Ewing's sarcoma formation, and that VEGF signaling plays a role in the chemoattraction of BM cells to the tumor area.

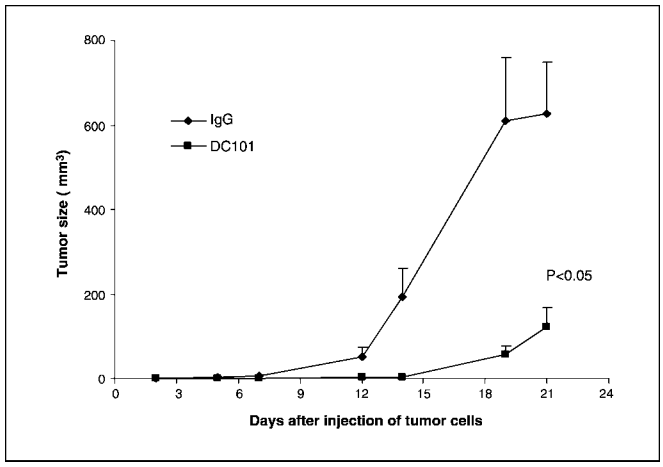

Fig. 1. DC101 inhibited the growth of Ewing's sarcoma tumors *in vivo*. TC71 cells were s.c. injected into H-2^d mice that had previously received transplanted BM cells from H-$2^{b/d}$ mice. The recipient mice were then treated with DC101 antibody or with (IgG_2 as control) i.p. twice weekly for 3 wks starting 3 d after tumor cell inoculation. Tumor size was quantified. Points, means from 10 mice; error, SD.

Materials and Methods

Cell lines. TC71 human Ewing's sarcoma cells were cultured in EMEM with 10% fetal bovine serum, 2 mmol/L L-glutamine, 1 mmol/L sodium pyruvate, 1× nonessential amino acids, and 2× MEM vitamin solution (Life Technologies, Inc.). Human femoral artery endothelial cells (HFAEC) were purchased from the American Type Culture Collection, and human microvascular endothelial cells (HMVEC) were purchased from Cambrex. These cells were cultured according to the instruction provided by the company. Mouse lung vessel endothelial cells (MLVEC) were kindly provided by Dr. Robert Langley (Department of Cancer Biology, The University of Texas M.D. Anderson Cancer Center, Houston, TX). Human $CD34^+$ stem cells were isolated from human umbilical cord blood as previously described (6). All of the cells were negative for *Mycoplasma*, as determined with a *Mycoplasma* PCR-ELISA kit (Roche Applied Science).

Reverse transcription-PCR. Total RNA was extracted from the different cells. The cDNA was synthesized using a reverse transcription (RT) system (Promega Corp.). RT products were amplified by PCR using specific primers for human VEGFR-2 (sense, 5′-GTGACCAA-CATGGAGTCGTG-3′; antisense, 5′-TGCTTCACAGAAGACCATGC-3′) and mouse VEGFR-2 (sense, 5′-TTCTGGACTCTCCCTGCCTA-3′; antisense, 5′-TCTGTCTGGCTGTCATCTGG-3′). The primers of VEGFR-1 for both human and mouse were obtained from R&D Systems. The initial denaturation was done at 94°C for 5 min. The products were then subjected to denaturation at 94°C for 1 min, annealing at 55°C for 1 min, extension at 72°C for 1 min (30 cycles), and a final elongation at 72°C for 10 min. Finally, the PCR products were subjected to electrophoresis on a 2% agarose gel with ethidium bromide and visualized under UV light.

***Human and mouse endothelial cell migration assay* in vitro.** Transwells (Costar) were pretreated with serum-free medium at 37°C for 1 h before being seeded with HMVECs or MLVECs at 1×10^5 per well in 100 μL medium with 0.1% fetal bovine serum. The Transwells were then inserted into 24-well plates containing 600 μL of medium. Recombinant human $VEGF_{165}$ (StemCell Technologies) at 200 ng/mL, DC101 antibody, or VEGFR-1 antibody MF-1 (ImClone Systems, Inc.) at 200 ng/mL, a combination of VEGF, or the same amount of nonrelated immunoglobulin G (IgG, as a control) was added to the medium in different wells. The Transwells were incubated at 37°C for 6 h to allow the cells to migrate. Cells on the upper side of the filter were then removed with cotton swabs, and the migrated cells on the lower side of the filter were fixed and stained with H&E. The number of migrated cells was counted using a binocular microscope. The average number of migrated cells was calculated from five random high-power microscopic fields.

Mouse model of MHC-mismatched BM transplantation in Ewing's sarcoma. Male nude BALB/cAnN mice with the MHC strain-specific surface antigen d (H-2^d) and C57BL × BALB/c F1 (CB6 F1) mice (H-$2^{b/d}$), 8 to 13 weeks old, were purchased from the National Cancer Institute. The mice were maintained in a specific pathogen-free animal facility approved by the American Association for Accreditation of Laboratory Animal Care and in accordance with current regulation and standards of the U.S. Department of Agriculture, the Department of Health and Human Service, and the NIH. The animal experiment protocol was approved by the Institutional Animal Care and Use Committee. The CB6 F1 mice (H-$2^{b/d}$) were used as the BM donors, and the BALB/cAnN mice (H-2^d) were used as the BM recipients.

BM transplantation was done as previously described (5). Briefly, the recipient mice were first whole-body irradiated using an external cesium source (^{137}Cs Mark 1 irradiator, J.L. Shepherd & Associates) with 8.0 Gy. Freshly isolated BM cells (10^6/200 μL) flushed from the femurs of CB6 F1 mice were injected via the lateral tail vein into the nude BALB/cAnN recipients within 2 h of their irradiation. Engraftment was confirmed with analysis using strain-specific H-2 surface antigens for donor interleukin-1β in the spleen and peripheral blood mononuclear cells (5).

Chimeric mice were injected s.c. with 3×10^6 TC71 cells in 100 μL of HBSS 4 weeks after BM transplantation. Tumors of 3 to 4 mm in diameter were detectable 6 days after injection of the TC71 cells.

Treatment of tumors with DC101. DC101 anti-mouse VEGFR-2 antibodies were generated as described previously (12). Mice (10 per group) were treated i.p. with DC101 or IgG (control) 800 μg per mouse, twice weekly for 3 weeks starting 3 days after their inoculation with the tumor cells. Tumor diameter was measured twice weekly with calipers. Tumor volumes were calculated using the formula $\frac{1}{2}ab^2$, in which a is the longer diameter, and b is the shorter diameter, and the volume is expressed in cubic millimeters. The mice were euthanized 3 weeks after the beginning of antibody treatment. Tumor tissue was collected from each mouse and analyzed by immunohistochemical staining for H-$2K^b$, CD31, alpha smooth muscle actin (α-SMA), and VEGFR-2 expression.

Immunofluorescence staining in tumor tissues. Rat anti-mouse CD31 and biotinylated mouse anti-mouse H-$2K^b$ antibodies were purchased from BD Biosciences PharMingen. α-SMA antibody was obtained from Abcam Inc. VEGFR-2 antibody was purchased from Sigma Co.

Tumor tissues were harvested from the mice in the different groups, and frozen sections were fixed with acetone and chloroform. Incubation in 4.5% fish gelatin (BB International Co.) for 20 min was used to block nonspecific proteins. Expression of CD31 was detected in blood vessels using rat anti-mouse CD31 as the primary antibody and goat anti-rat TexasRed (Jackson) as the secondary

antibody. The mean MVD was determined by first counting and then averaging the number of CD31-positive cells in five random high-power microscopic fields from different tumors. For double fluorescence staining, the sections were incubated with an avidin-biotin blocking kit (Vector Laboratories), and then H-2K^b was used as the primary antibody and streptavidin-FITC (BD Biosciences) as the second antibody.

Terminal nucleotidyl transferase–mediated nick end labeling assay. Terminal nucleotidyl transferase–mediated nick end labeling (TUNEL) assay was done to detect apoptotic cells. DeadEnd Fluorometric TUNEL System Kit was purchased from Promega Co. TUNEL staining in frozen tumor tissues was done according to instruction provided by the company. The green fluorescence of apoptotic cells was detected using a fluorescence microscope. The average number

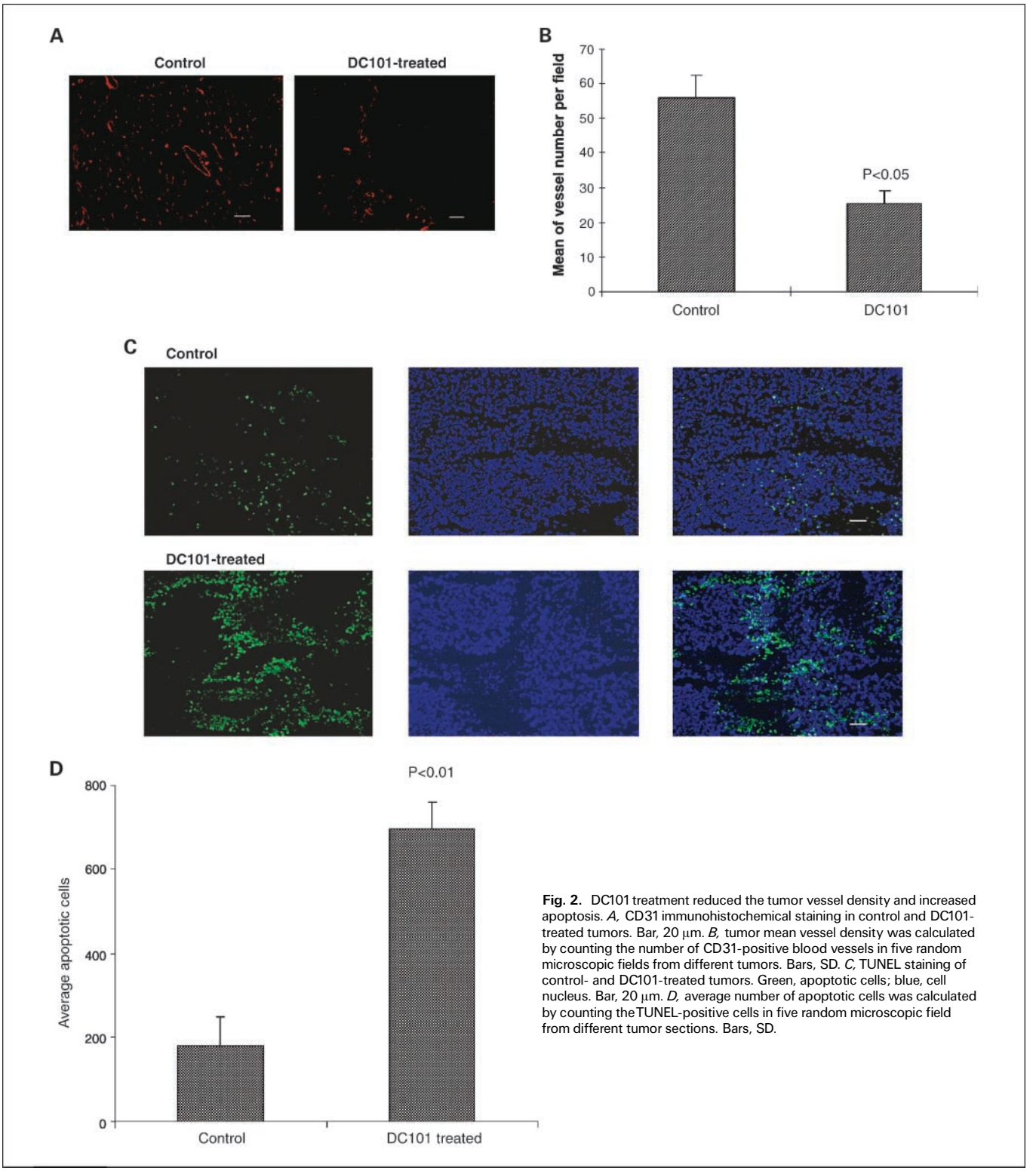

Fig. 2. DC101 treatment reduced the tumor vessel density and increased apoptosis. *A,* CD31 immunohistochemical staining in control and DC101-treated tumors. Bar, 20 μm. *B,* tumor mean vessel density was calculated by counting the number of CD31-positive blood vessels in five random microscopic fields from different tumors. Bars, SD. *C,* TUNEL staining of control- and DC101-treated tumors. Green, apoptotic cells; blue, cell nucleus. Bar, 20 μm. *D,* average number of apoptotic cells was calculated by counting the TUNEL-positive cells in five random microscopic field from different tumor sections. Bars, SD.

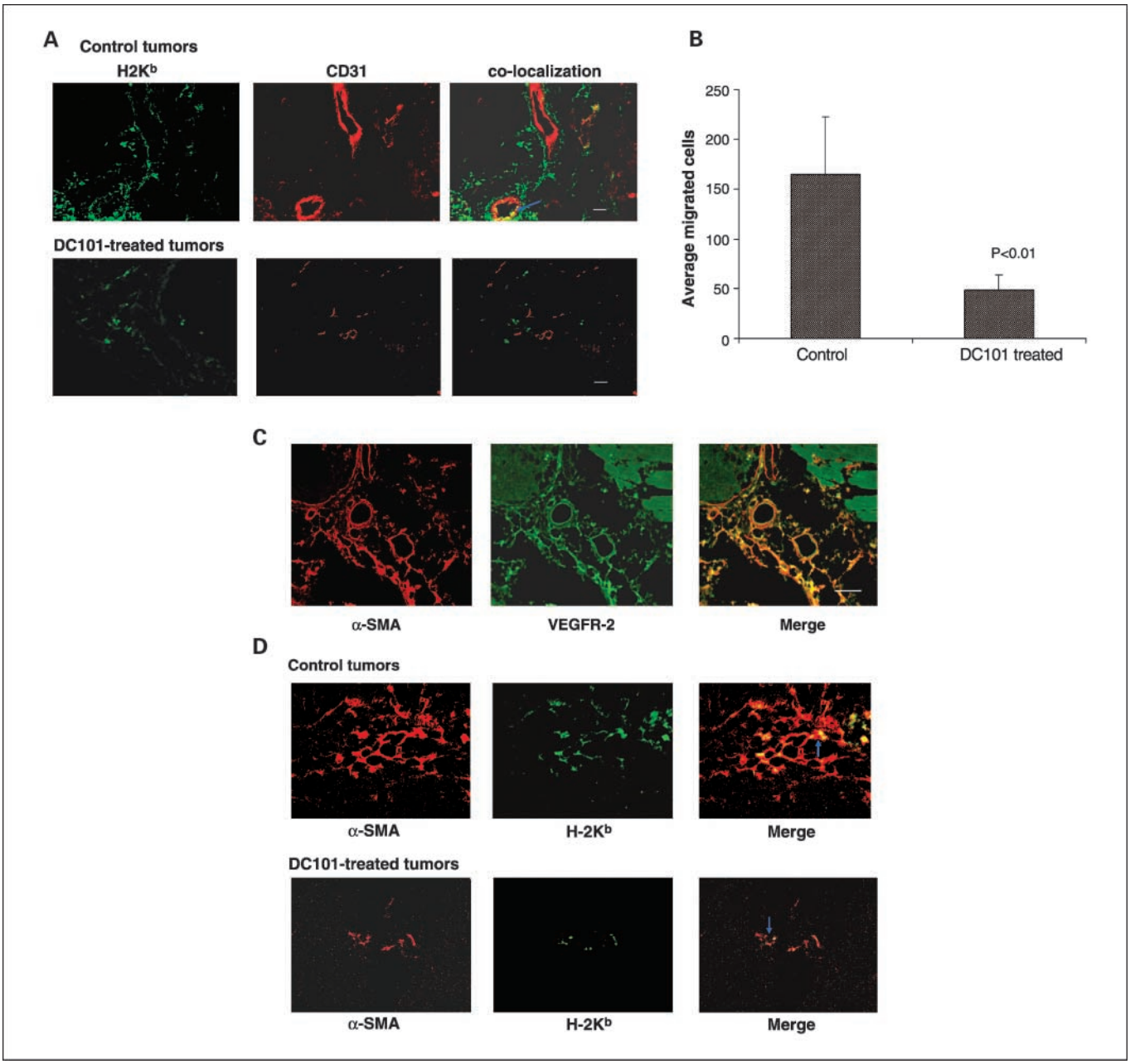

Fig. 3. Effect of DC101 on migration of BM cells into the tumor area. *A,* double immunofluorescence staining for H-2K^b (*green*) and CD31 (*red*) in control and DC101-treated tumor tissues. Yellow, colocalization of both stains (*arrow*), therefore indicating that donor BM cells that migrated into the tumor participated in tumor vessel formation. Bar, 20 μm. *B,* the average number of migrated cells was calculated by counting the H2K^b-positive cells in five random microscopic field from different tumor section. Bars, SD. *C,* VEGFR-2 expression in tumor vessel pericytes. Pericyte marker α-SMA (*red*) and VEGFR-2 (*green*) double immunofluorescence staining was shown in the control tumors. Yellow, cells that express both VEGFR-2 and α-SMA. Bar, 20 μm. *D,* effect of DC101 on tumor pericytes. Pericyte marker α-SMA (*red*) and BM cell marker H-2K^b (*green*) double immunofluorescence staining (*yellow*) indicates pericytes derived from BM cells. The number of such cells was substantially reduced in DC101-treated tumors.

of apoptotic cells in control and DC101-treated tumors was calculated by counting the number of TUNEL-positive cells in five random microscopic fields from different tumors.

Statistical analysis. The two-tailed Student's *t* test was used to compare the tumor volumes and numbers of blood vessels for the different treatment groups. A *P* value of <0.05 was considered statistically significant.

Results

Effect of DC101 antibody therapy on tumor growth and tumor MVD. Nude BALB/c mice (H-2^d) underwent BM transplantation with cells from the CB6F1 (H-2$^{b/d}$) donor mice. Four weeks after the transplantation, the chimeric mice were injected with TC71 cells s.c. Therapy with DC101 or IgG was initiated twice weekly for 3 weeks starting 3 days after tumor cell inoculation. DC101 antibody therapy significantly suppressed tumor growth compared with IgG therapy (Fig. 1, $P < 0.05$), suggesting that suppression of VEGFR-2 inhibits tumor growth.

Immunofluorescent CD31 staining of tumor tissues (Fig. 2A) was used to quantify tumor MVD. CD31 expression was also significantly decreased in the DC101-treated tumors. The tumor MVD (Fig. 2B) in the DC101-treated group was 25 ± 4 vessel

number per field, compared with 56 ± 7 vessel number per field in the control group ($P < 0.05$). The tumor vessel morphology was also different in the control and DC101-treated tumors. The control-treated tumors contained numerous tortuous large vessels. By contrast, the majority of tumor vessels in the DC101-treated tumors were smaller and less tortuous. TUNEL staining detected large areas of apoptosis throughout the DC101-treated tumors compared with the IgG-treated control tumors (Fig. 2C). The average number of apoptotic cells in DC101-treated tumors was significantly increased compared with that in control tumors (Fig. 2D).

Localization of donor BM cells in the new vessels of Ewing's sarcoma tumors. We previously showed that BM cells migrate to Ewing's sarcoma tumors and incorporate into the expanding tumor vessels that support tumor growth (5). The presence of donor-cell–derived H-2K^b–positive vessels and stromal cells was assessed in treated and control tumors. Numerous H-2K^b–positive tumor vessels and cells within the tumor stroma were observed in the control tumors. Colocalization of H-2K^b (green) and CD31 (red) by double-immunofluorescence staining (Fig. 3A) confirmed that BM-derived cells participate in tumor vessel formation. In contrast, fewer H-2K^b–positive donor cells (green) were seen in the DC101-treated tumors. The average number of migrated BM-derived cells was significantly reduced in DC101-treated tumors compared with the control tumors (Fig. 3B). The number of double-stained positive cells was also decreased.

To determine whether tumor vessel pericytes express VEGFR-2, we did double immunofluorescence staining using the pericyte marker α-SMA and VEGFR-2. Colocalization of VEGFR-2 and α-SMA was observed in numerous areas of the tumors (Fig. 3C). The α-SMA (red) and H-2K^b (green) double immunofluorescence staining (Fig. 3D) showed that many of these pericytes were donor derived (i.e., H-2K^b positive), indicating that these cells originated from the BM and migrated to the tumors (yellow area, see arrow). The number of cells expressing both H-2K^b and α-SMA and the overall area showing coexpression of these two markers were decreased in DC101-treated tumors compared with control tumors. These results suggest that DC101 not only inhibited migration of

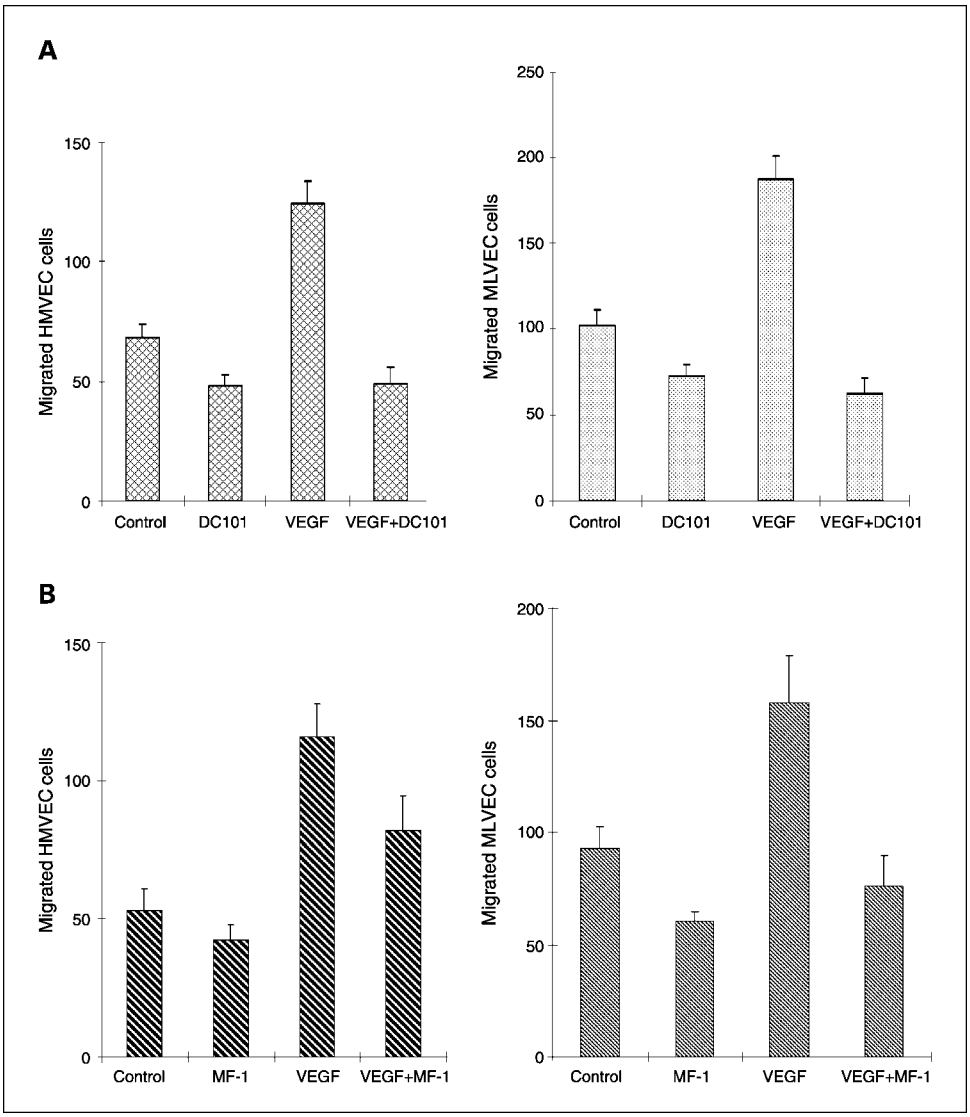

Fig. 4. Effect of DC101 or MF-1 on migration of human and mouse endothelial cells *in vitro*. *A,* the effect of VEGFR-2 antibody DC101 on migration of endothelial cells. HMVEC (*left*) or MLVEC (*right*) were set in Transwells, which were then inserted into a 24-well plate containing medium alone or medium with DC101, recombinant human VEGF, or both. The average number of cells that migrated was calculated from the counts in five random high-power microscopic fields. Bars, SD. *B,* the effect of VEGFR-1 antibody MF-1 on migration of endothelial cells.

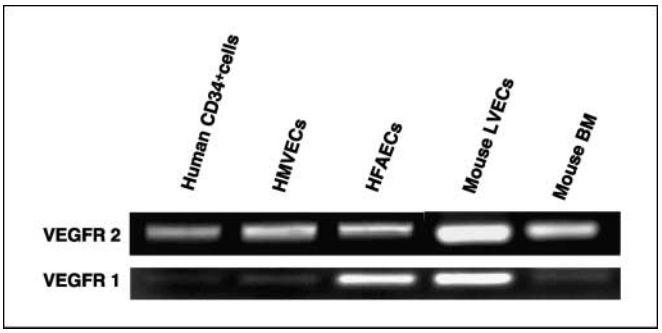

Fig. 5. VEGFR-2 and VEGFR-1 expression in human and mouse cells. Total RNA was extracted from different cells, and RT-PCR analysis was done. LVECs, lung vessel endothelial cells.

BM-derived cells into the tumors, but also inhibited BM-derived pericyte formation in the tumor vessels.

***Effect of DC101 on endothelial cell migration* in vitro.** The effect of DC101 on migration of HMVECs and MLVECs *in vitro* was evaluated using Boyden chambers. DC101 significantly inhibited VEGF-induced migration of both cell lines (Fig. 4A). This result was as we expected because both HMVECs and MLVECs express VEGFR-2 (Fig. 5). Similarly, mouse BM and human $CD34^+$ cells expressed VEGFR-2. The expression of VEGFR-1 was variable depending on the cell line (Fig. 5).

We also investigated the effect of blocking VEGFR-1 on endothelial cell migration. Similar to DC101, MF-1 inhibited the migration of both HMVECs and MLVECs *in vitro* (Fig. 4B).

Discussion

We previously showed that Ewing's sarcoma cells overexpress the soluble $VEGF_{165}$ isoform, BM-derived cells chemotax to $VEGF_{165}$-containing Matrigel plugs *in vivo*, and that these BM-derived cells contribute to the expansion of the growing tumor vascular network (5, 6). We further showed that $VEGF_{165}$ is critical to the growth of Ewing's sarcoma tumors *in vivo* (6, 11). Specifically inhibiting this isoform decreased BM-derived cell infiltration, tumor vessel development, and tumor growth. Taken together, these data indicate that VEGF may be a therapeutic target for the treatment of patients with Ewing's sarcoma.

VEGF exerts its biological functions on endothelial cells through two receptors: VEGFR-2 (Flk-1/KDR) and VEGFR-1 (Flt-1), although VEGFR-2 is considered to be more dominant (13). Here, we showed that treatment with an antibody directed against VEGFR-2 resulted in the inhibition of tumor growth and decreased tumor vessel density. The recruitment of BM-derived cells into the tumor area was also severely decreased in the tumors treated with anti–VEGFR-2 antibody. The mechanism by which tumors attract BM-derived cells to the tumor area and the chemoattractants involved are not fully understood. VEGF has been shown to be a potent chemotactic factor for BM cells (14) and to induce colony formation by progenitor cells. We have previously shown that Ewing's tumor cells and patient tumor specimens express high levels of VEGF (11, 15). We have further shown that there is a switch from the extracellular matrix–bound 189 isoform to the more soluble 165 isoform of VEGF (6). We hypothesize that this isoform switching favors an increase in secreted VEGF, which in turn results in the recruitment of BM-derived cells to the tumor area. The data presented here show that interference with VEGFR-2 blocks the chemotaxis of BM-derived cells in addition to inhibiting tumor growth and tumor vessel development. Thus, once again, we have shown a link between the recruitment of BM-derived cells, tumor vessel development, and tumor growth, strengthening our hypothesis that a postnatal vasculogenesis-like mechanism, in addition to angiogenesis, plays an important role in the growth of Ewing's sarcoma.

Blood vessel pericytes also play a critical role in tumor vessel formation. The BM is a reservoir of pericyte progenitors (16). Our data showed that a portion of the tumor vessel pericytes were $H\text{-}2K^b$ positive (Fig. 3D), indicating that they were BM derived. However, whether these cells migrated into the tumor and then differentiated into pericytes or had already differentiated before arriving in the tumor is unclear. We further showed that tumor-associated pericytes expressed VEGFR-2, and that DC101 treatment not only inhibited BM-derived cell chemotaxis and tumor vessel formation, but also inhibited pericyte formation on the tumor vessels.

VEGFR-2 is an attractive target for antitumor therapy. Previous studies have focused on the effects of VEGFR-2 therapy on tumor angiogenesis. Evidence is increasing that, in addition to angiogenesis, postnatal vasculogenesis is involved in neovascularization during tumor growth. Recent reports have indicated that bolus chemotherapy, such as with cyclophosphamide, leads to acute recruitment of circulating endothelial progenitor cells to the tumor (17, 18), and that there is a correlation with the number of circulating progenitor cells and patient outcome (19, 20). Thus, these endothelial progenitor cells may serve to rescue the tumor by providing cells that can form new tumor vessels.

In summary, we have shown that targeting VEGFR-2 may interfere with vasculogenesis by preventing BM-derived cell migration into the tumors. Combining VEGFR-2–targeted agents with chemotherapy may therefore improve the efficacy of treatment by interfering with the ability of BM progenitor cells to repair damaged tumor vessels and restore the necessary vascular supply. Our data indicate that such an approach may be effective in Ewing's sarcoma because we have already shown the importance of postnatal vasculogenesis during tumor growth. The survival rate for patients with Ewing's sarcoma has remained stagnant for 20 years, hovering at about 40% to 50%. Therefore, it behooves us to consider novel therapeutic approaches such as the one studied here.

References

1. Holash J, Maisonpierre PC, Compton D, et al. Vessel cooption, regression, and growth in tumors mediated by angiopoietins and VEGF. Science 1999;284:1994–8.
2. Maniotis AJ, Folberg R, Hess A, et al. Vascular channel formation by human melanoma cells *in vivo* and *in vitro*: vasculogenic mimicry. Am J Pathol 1999;155:739–52.
3. Sharma N, Seftor RE, Seftor EA, et al. Prostatic tumor cell plasticity involves cooperative interactions of distinct phenotypic subpopulations: role in vasculogenic mimicry. Prostate 2002;50:189–201.
4. Sood AK, Seftor EA, Fletcher MS, et al. Molecular determinants of ovarian cancer plasticity. Am J Pathol 2001;158:1279–88.
5. Bolontrade MF, Zhou RR, Kleinerman ES. Vasculogenesis plays a role in the growth of Ewing's sarcoma *in vivo*. Clin Cancer Res 2002;8:3622–7.
6. Lee TH, Bolontrade MF, Worth LL, Guan H, Ellis LM, Kleinerman ES. Production of $VEGF_{165}$ by Ewing's sarcoma cells induces vasculogenesis and the incorporation of $CD34^+$ stem cells into the expanding tumor vasculature. Int J Cancer 2006;119:839–46.

7. Folkman J. Angiogenesis in cancer, vascular, rheumatoid and other disease. Nat Med 1995;1:27–31.
8. Ferrara N. Vascular endothelial growth factor as a target for anticancer therapy. Oncologist 2004;9:2–10.
9. Greenberg DA, Jin K. From angiogenesis to neuropathology. Nature 2005;15:954–9.
10. Tsuchihashi S, Ke B, Kaldas F, et al. Vascular endothelial growth factor antagonist modulates leukocyte trafficking and protects mouse livers against ischemia/reperfusion injury. Am J Pathol 2006;168:695–705.
11. Guan H, Zhou Z, Wang H, Jia SF, Liu W, Kleinerman ES. A small interfering RNA targeting vascular endothelial growth factor inhibits Ewing's sarcoma growth in a xenograft mouse model. Clin Cancer Res 2005;11:2662–9.
12. Shaheen RM, Ahmad SA, Liu W, et al. Inhibited growth of colon cancer carcinomatosis by antibodies to vascular endothelial and epidermal growth factor receptors. Br J Cancer 2001;17:584–9.
13. Kowanetz M, Ferrara N. Vascular endothelial growth factor signaling pathway: therapeutic perspective. Clin Cancer Res 2006;12:5018–22.
14. Moore MA, Hattori K, Heissig B, et al. Mobilization of endothelial and hematopoietic stem and progenitor cells by adenovector-mediated elevation of serum levels of SDF-1, VEGF and angiopoietin-1. Ann N Y Acad Sci 2001;938:36–45.
15. Zhou Z, Zhou RR, Guan H, Bucana CD, Kleinerman ES. E1A gene therapy inhibits angiogenesis in a Ewing's sarcoma animal model. Mol Cancer Ther 2003;2:1313–9.
16. Lamagna C, Bergers G. The bone marrow constitutes a reservoir of pericyte progenitors. J Leukoc Biol 2006;80:1–5.
17. Bertolini F, Paul S, Mancuso P, et al. Maximum tolerable dose and low-dose metronomic chemotherapy have apposite effects on the mobilization and viability of circulating endothelial progenitor cells. Cancer Res 2003;63:4342–6.
18. Shaked Y, Charrocchi A, Franco M, et al. Therapy-induced acute recruitment of circulating endothelial progenitor cells to tumors. Science 2006;313:1785–7.
19. Mancuso P, Colleoni M, Calleri A, et al. Circulating endothelial-cell kinetics and viability predict survival in breast cancer patients receiving metronomic chemotherapy. Blood 2006;108:452–9.
20. Bertolini F, Shaked Y, Mancuso P, Kerbel RS. The multifaceted circulating endothelial cell in cancer: towards marker and target identification. Nat Rev Cancer 2006;6:835–45.